Inverse Modeling of the Deep Brazil Basin Circulation

Garrett Finucane

garrettf@uw.edu

Abstract

The pathways of seawater through the deepest parts of the world ocean are relatively unknown but critical to understanding how the ocean distributes heat that is taken up at the surface. The deep and abyssal circulation across 30°S in the Brazil Basin is inferred from multiple decades of full-depth CTD data by a potential vorticity and salt conserving inverse model which parameterizes diapycnal mixing as a function of bathymetric roughness. The basin exhibits strong diapycnal mixing especially towards its boundaries, and weak lateral mixing. The largest transport outside of boundary currents across 30°S is the southward flow of Antarctic Bottom Water (AABW) at a rate of ~10^{10} kg s^{-1}. AABW flows northward through the Vema Channel and southward in the interior of the basin creating a cyclonic circulation around the Rio Grande Rise. Flow along -30°S is westward in the Antarctic Intermediate Water (AAIW) and Upper Circumpolar Deep Water (UCDW), and eastward in the North Atlantic Deep Water (NADW).

Plain Language Summary

While the circulation of the surface ocean is relatively well known, the mean flow of the ocean's deepest waters is not as well understood. Better understanding how water moves around deep in the ocean is a crucial part of understanding how the ocean will respond to a rapidly changing climate. Directly measuring the deep circulation is difficult because to do so requires installing many instruments thousands of meters deep and having them record data for a very long time. Instead, inverse models, like the one presented in this study, use decades of measurements taken from ships to map temperature and salinity across a basin, and infer how water must be flowing to establish those patterns. In this study an inverse model is used to find how water flows in the deep parts of the ocean basin off the coast of Brazil. The model results show that the majority of water which is transported across 30°S, away from the

edges of the basin, is the Antarctic Bottom Water flowing southward. The model also finds that the Brazil Basin has relatively high rates of mixing which is consistent with the work of previous studies in the basin.

Introduction

Heat and CO_2 which the ocean absorbs at the surface makes its way throughout the deep ocean over decades to centuries. Understanding how the heat that is taken up at the surface is transported through the world's oceans is crucial to understanding how the world ocean will change in the future. Finding the mean deep circulation by direct observation is possible, but in practice very difficult due to the spatial resolution and duration needed to observe more than the instantaneous eddy field. Instead of measuring the mean circulation directly, inverse techniques observe the existing patterns of salinity, temperature, and potential vorticity along neutral surfaces and ask what circulation must exist for such patterns to arise. While salinity and potential vorticity are largely conservative tracers, diapycnal mixing slowly homogenizes salinity and acts as a sink of potential vorticity by reducing stratification. In the deep ocean, rough bathymetry may drive diapycnal mixing that is significant enough that it must be taken into account in order to correctly infer the mean circulation. Hautala (2018) employed an inverse method, based on salinity and potential vorticity conservation equations, which parameterizes diapycnal mixing as a function of bathymetric roughness and height above the seafloor (Kunze et al. 2006) in order to infer the mean circulation of the Northeast Pacific Basin. Unlike classical box inverse models, which attempt to conserve the mass of water leaving and entering the basin by solving for the velocity at the boundary of the domain (Wunsch 1978), this method lays a grid over the interior of the domain and conserves potential vorticity throughout it. This study applies this method to the western Brazil Basin in order to gain a better understanding of the flow of Antarctic Intermediate Water (AAIW), Upper Circumpolar Deep Water (UCDW), North Atlantic Deep Water (NADW), and Antarctic Bottom Water

(AABW) throughout the Brazil Basin. In particular, this work seeks to answer which of the three inverse methods presented in Hernandez-Guerra et al. (2019) is most consistent with interior potential vorticity conservation given the inhomogeneous deep mixing field of the Brazil Basin.

The western Brazil Basin has been chosen for this study due to the wealth of data collected and research conducted there, as well as for the open questions about the basin's deep and abyssal circulation. There is an abundance of existing high-quality, full-depth CTD data that has been taken as a part of the WOCE, and subsequent CLIVAR and GO-SHIP repeat hydrography programs (Figure 1). This hydrographic data allows for the creation of accurate full depth maps of salinity and potential vorticity throughout the basin which is a prerequisite for the inverse method. In addition to hydrographic

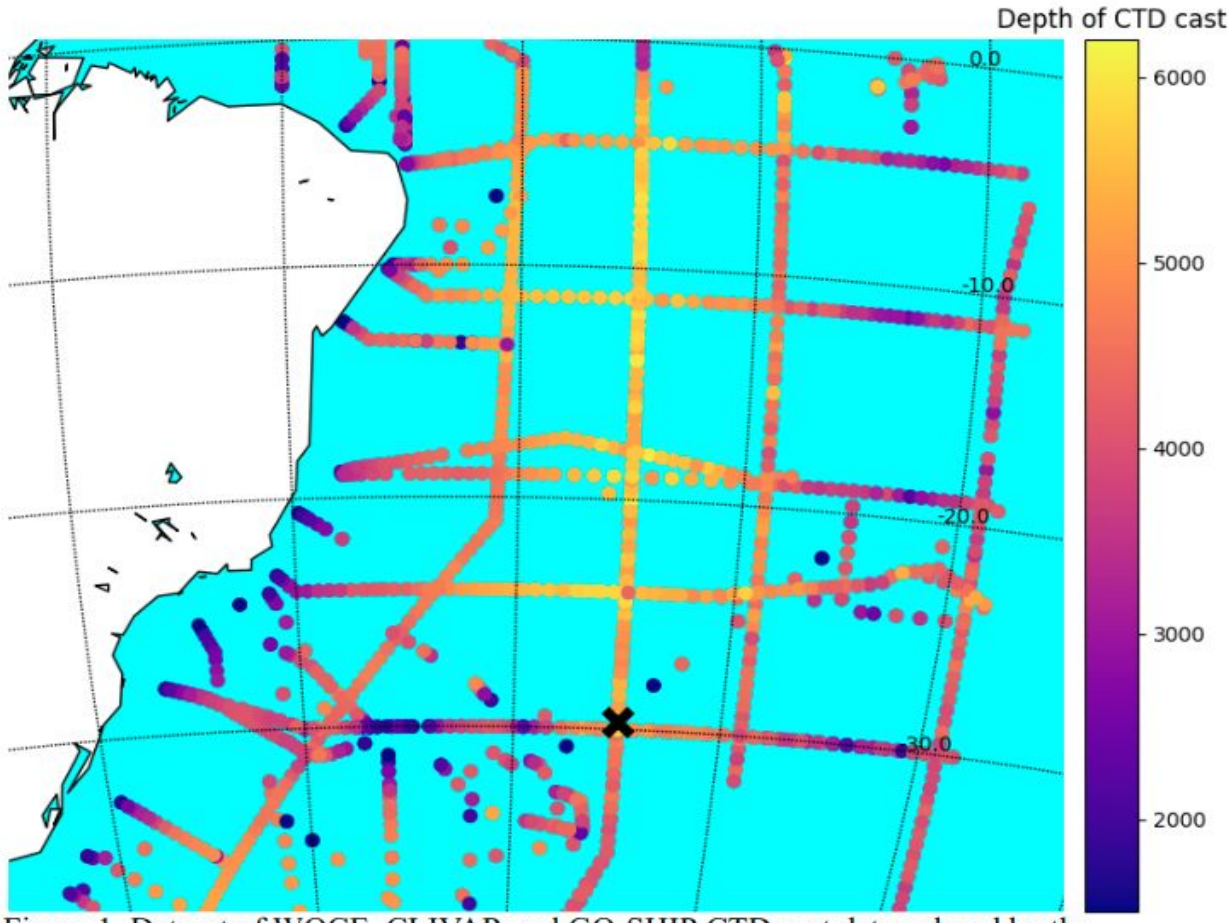

Figure 1. Dataset of WOCE, CLIVAR and GO-SHIP CTD cast data colored by the maximum depth of data collected. Reference cast marked by black x.

data, direct measurements of the diapycnal diffusivity of the abyssal Brazil Basin have been made (Polzin et al. 1997). An inverse model using these direct measurements has also been conducted but restricted its domain to the region to near where diapycnal diffusivity had been measured (St. Laurent et al. 2001). Hernandez-Guerra et al. (2019) employed three separate inverse models in order to diagnose the transport across 30°S in the Brazil Basin. While one model (Model C) is a classical mass-conserving box inverse model which relies on hydrographic data to constrain mass transport, the other two (Models A and B) are constrained by previously determined transport estimates. Model A is constrained by transport estimates from Talley (2008) which are based on reference velocities adjusted from Reid (2004) that were carefully chosen to create flows which are congruent with tracer distributions observed in the ocean. Model B is constrained by transport estimates and standard deviations from the Southern Ocean State Estimate (Mazloff et al. 2010). To understand how these models differ with each other, and with results from observational studies, the main water masses in the region, the Antarctic Intermediate Water (AAIW), Upper Circumpolar Deep water (UCDW), North Atlantic Deep Water (NADW), and Antarctic Bottom Water (AABW), must be differentiated.

AAIW sits at about 900m in the southern Brazil Basin and is characterized by a salinity minimum, and σ_1 values between 31.53 kg/m^3 and 31.98 kg/m^3 (Peterson 1992). Boebel et al. (1997) deployed neutrally buoyant floats in combination

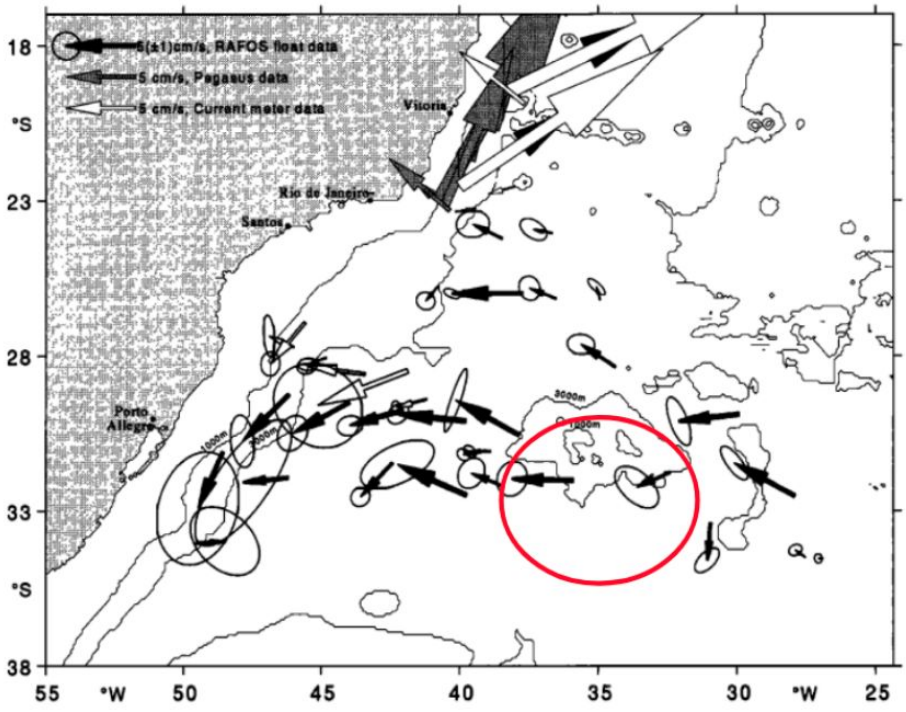

Figure 2. Average of float and current meter velocities in the AAIW from Boebel et al. (1997). Velocities show clear westward flow along 26°S until ~42°W at which point it splits north and south. The Rio Grande Rise is circled in Red.

with current meters in order to study the flow of AAIW across the Rio Grande Rise. The observed flow traveled west along 26°S until it reached 42°W at which point half turned north, and the other half turned south (Figure 2). These observations are consistent in direction with the inverse modelling efforts of Hernández-Guerra et al. (2019), but differ in magnitude. Boebel et al. (1997) estimated a -5.5 to -10.5 Sv flow across 30°S, while Hernandez-Guerra et al. (2019) found a transport of -4.0 to -6.3 Sv in 2003 and a significantly weaker -0.1 to -1.1 Sv transport in 2011.

UCDW lies between 1300 and 1550 m in the southwestern Brazil Basin and is characterized by an oxygen and temperature minimum, with a σ_1 value of about 32.20 kg/m^3 (Reid 1989). The UCDW is thicker than the AAIW along 30°S (Speer et al. 2000). The work of Reid (1989) and Muller (1998) suggest that the circulation of UCDW is similar schematically to AAIW. Hernandez-Guerra et al. (2019) found transports similar to work of Reid (1989) and Muller (1998).

NADW is characterized by high salinity (>34.85) and a silicate minimum. In the south western Brazil Basin it reaches from about 1600m to about 3400m depth (Reid 1989). Hogg and Owens (1999) deployed 99 neutrally buoyant floats to study NADW throughout the Brazil Basin (Figure 3). The authors found no consistent poleward component to the circulation, although they note that they did not release enough floats to

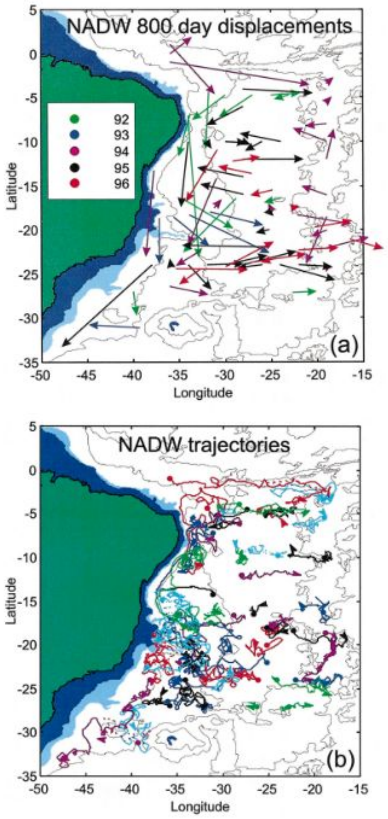

Figure 3. 800 day displacement and trajectories of neutrally buoyant floats released into NADW from Hogg and Owens (1999). The float data demonstrates the complexity of the deep circulation and the lack of clear meridional flow.

suitably capture the spatial complexity of the circulation. The surprising complexity of the floats' trajectories casts doubt on the classical theory of uniform poleward flow of deep and abyssal waters as predicted by Stommel (1957), which assumes uniform diapycnal mixing. It also paints a very different picture than the three inverse models presented in Hernandez-Guerra et al. (2019). While all three models show southward transport across 30°S they tell very different stories about the fate of NADW in the basin as a whole (Figure 4). While Model C shows a weak southward transport and DWBC west of the Mid Atlantic Ridge (MAR) that ramps up toward the eastern side of the basin, Model A and Model B show the majority of transport occurring in the western side of the basin that weakens across the Mid Atlantic Ridge.

AABW is classified as the water mass colder than 2°C, and fresher than 34.86 PSU (Reid 1989). Hogg and Owens (1999) deployed 69 neutrally buoyant floats to study the circulation of AABW. These floats paint a similar picture as the ones released in the NADW exhibiting mostly zonal movement with little consistent meridional flow. The three inverse models in Hernandez-Guerra et al. (2019) do not paint any clearer of a picture of

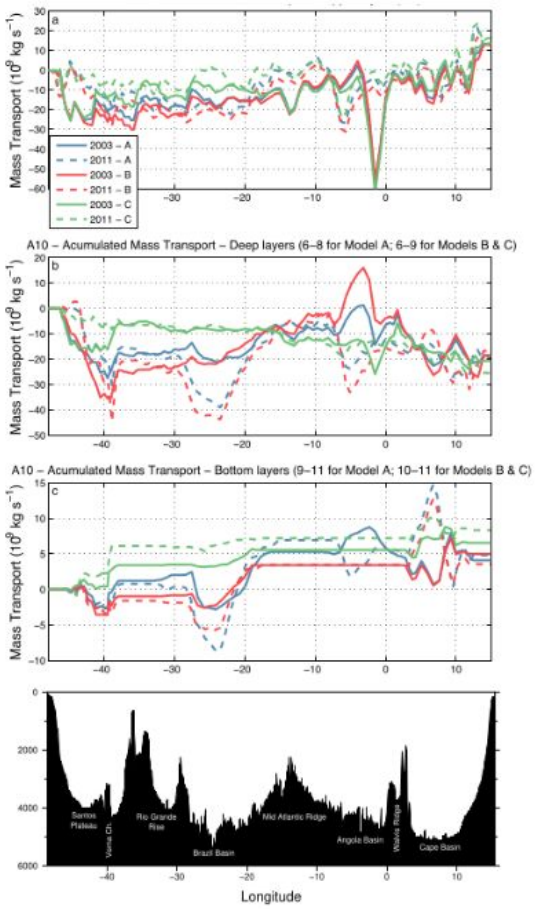

Figure 4. The transport across 30°S in the Brazil basin divided into three layers from three inverse models from Hernandez-Guerra et al. (2019), along with bathymetry along 30S.

the bottom water circulation between 40°W and 20°W. While Models A and B show strong southward transport of ~3 Sv at 40°W and ~5 Sv at 25°W, Model C shows a significantly more muted southward transport of ~ 0.5 Sv at 40°W and ~0 Sv at 25°W(Figure 4). A more regional attempt to determine the circulation around 30°S between 48°W and 34°W finds a complex snake-like circulation of alternating southward and northward transport (Figure 5**)** by calculating the geostrophic velocity along three WOCE hydrographic lines and referencing them to direct current measurements (McDonagh et al. 2002). It is important to note that underdetermined box inverse models like those of McDonagh et al. (2002) and Hernandez-Guerra et al. (2019) are very sensitive to their assumed integrated transport constraints. While the results of McDonagh et al. (2002) do not match any model presented in Hernandez-Guerra et al. (2019), they do show alternating northern and southern transports similar to Model A. This suggests that classical inverses like Model C in Hernandez-Guerra et al. (2019) are missing a key part of the circulation at 30°S.

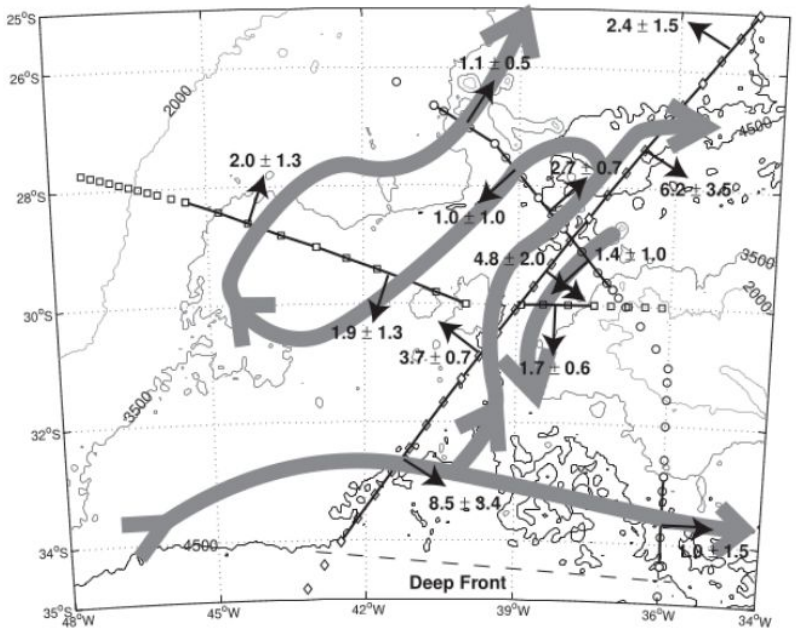

Figure 5. Transport of AABW between 48°W and 34°W around 30°S from McDonagh et al. (2002). This circulation schematic demonstrates the potentially complex snake-like nature of the flow near the Vema Channel.

We propose that classical mass conserving inverse models of this region are not considering the effect of potential vorticity conservation and bottom intensified diapycnal mixing in this region. Polzin et al. (1997) demonstrated the effect of bottom roughness on diapycnal mixing near the seafloor along the Mid-Atlantic Ridge in the Brazil Basin. Measurements of bathymetric roughness conducted by

Morris et al. (2001) show regions of high bathymetric roughness, and therefore high diapycnal mixing, around 30°S. Hogg and Owens (1999) suggest that the zonal component of the flow they observed was due to increased diapycnal mixing along the Mid-Atlantic Ridge flank. The inverse method employed by Hautala (2018) not only conserves potential vorticity, but parameterizes diapycnal mixing as a function of bottom roughness and distance from the seafloor (Kunze et al. 2006). It is expected that applying this inverse method to the Western Brazil Basin will result in better constrained flows of AABW in the interior of the basin, despite its inability to resolve powerful narrow Deep Western Boundary Currents (DWBC.)

Methods

The inverse model employed in this study is an adaptation of the inverse model of Hautala (2018). This inverse method evolved from the "beta-spiral" class of inverses that conserves potential vorticity and salinity. To begin, the model is fed 40 years of CTD data taken in the Brazil Basin and a single reference station from the Vema Channel is chosen for its depth and proximity to 30°S. Neutral density is calculated down the reference cast using the gamma_n package for Matlab and the pressure of each layer as defined by Hernández-Guerra et al. (2019) is found. This inverse contains more layers than the ten found in Hernández-Guerra et al. (2019), but they are chosen to lie near the layers of that study so as to allow for direct comparison of transport values. Using this reference station, neutral depths are found throughout the basin by solving the dianeutral relation (Jackett and Mcdougall 1997) identically to Hautala (2018). The spatial distribution of salinity, temperature, salinity and pressure is then mapped along these surfaces using a thin-plate spline Generalized Additive Model (GAM) interpolation which models complex functions as the addition of simpler smooth ones (Trossman et al. 2011). A 1° x 1° grid is then laid over the domain and a system of equations based on salinity and potential vorticity conservation is formed in which the values of the reference stream function at each grid point, along

with free parameters in the mixing functions, are the unknowns. Using singular value decomposition the least squares solution to this overdetermined system of equations is found, along with information about the matrix condition which is useful in determining the maximum number of free parameters for the mixing coefficients that can be resolved by the linear system of equations. Diapycnal diffusivity is parameterized as:

$$K_V = j(N/f)\left[K_{V0} + K_{VB}\left(\frac{var(D)}{var(D)_0}\right)^{1/4} e^{-(D-p)/H_0}\right]$$

Where K_{V0} is a single value throughout the basin, and K_{VB} is solved for each grid point. At a grid point, D is the depth of the seafloor, p is the pressure of the grid point, and H_0 is the decay scale of diapycnal mixing with distance from the seafloor. For a more in depth discussion of this method see Hautala (2018).

This implementation of the inverse method does differ in some small ways from Hautala (2018). First, the whole method was rewritten as a Python library in order to make it more extensible. This Python implementation was then run on the same Northeast Pacific Basin data as the original Matlab software and verified to yield the same results. Second, the number of splines used by the GAM interpolation was chosen to minimize the neutrality error of the surfaces constructed. Third, the column weighting of the spatially dependent vertical mixing coefficient (KV_b) was chosen to be 10^{-2} m^2 s^{-1} instead of its value of 5×10^{-5} m^2 s^{-1} in the Northeast Pacific Basin as this greatly reduced both the condition and error of the solution. This difference is a reflection of the increased importance of diapycnal mixing due to bathymetric roughness in the Brazil Basin compared to the relatively quiescent Northeast Pacific Basin. Finally, unlike in Hautala (2018) no manual salinity correction was applied to the CTD profiles. The preferred inverse solution that reflects all of these changes is denoted Run 0.

Results

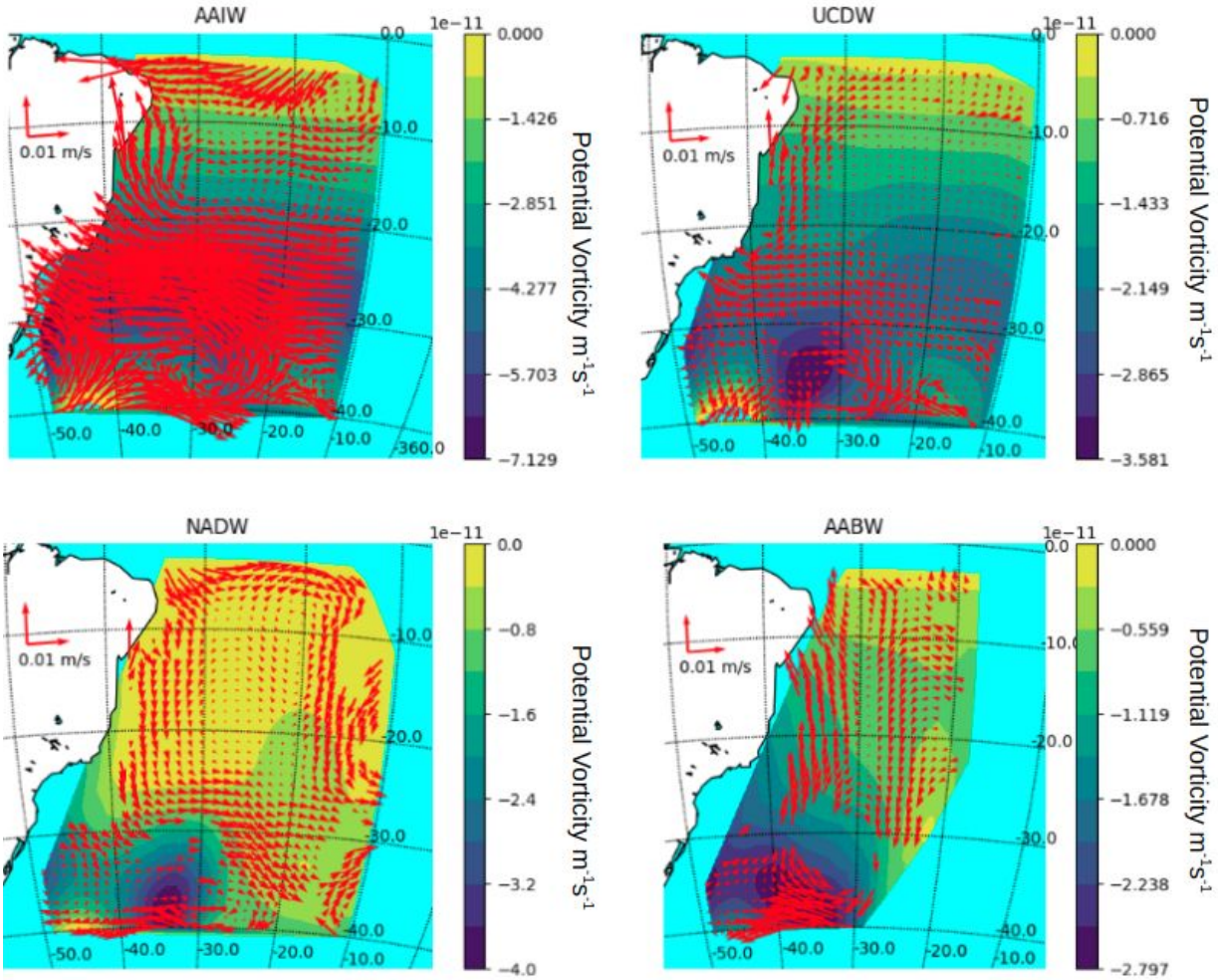

Figure 6. Absolute geostrophic velocity in AAIW (γ^n = 27.48), UCDW (γ^n =27.89), NADW (γ^n = 28.07), and AABW (γ^n = 28.19). Potential vorticity is contoured in the background. Reference arrows are shown for scale on the continent.

n

Lateral circulation

The flow of AAIW and UCDW in the southern half of the basin is predominantly eastwards north of 30°S, largely following gradients of potential vorticity in the interior of the basin (Figure 6). The western boundary currents expected along the South American continental slope are unresolved by

this inverse method. In the NADW, circulation becomes predominantly eastward along 30°S. In the AABW, northward transport through the Vema Channel pairs with a southward flow east of 30°W to create a cyclonic circulation around the Rio Grande Rise.

Mixing

The average value of diapycnal diffusivity K_V throughout all surfaces below 1000 dbar and above 4200 dbar is 2.0 x 10^{-5} m^2 s^{-1}. Run 0's basin wide diapycnal mixing coefficient K_{V0} = -3.15 x 10^{-5} m^2 s^{-1}, and the basin wide average of the spatially dependent coefficient of diapycnal mixing K_{VB} = 2.0 x10^{-4} m^2 s^{-1}. The average value of lateral mixing (K_H), which is solved for on each layer, is 80 m^2 s^{-1}. Diapycnal mixing is low in the interior of the basin, and increases towards the edges (Figure 7).

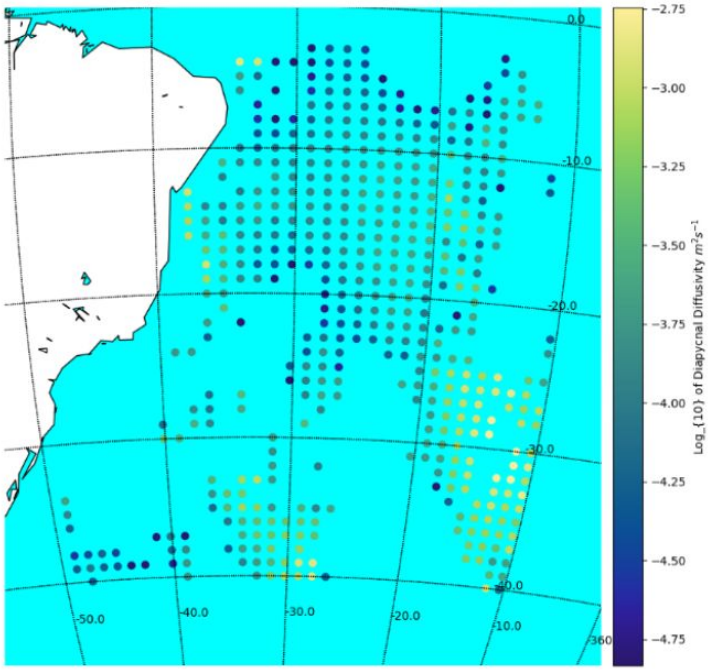

Figure 7. Diapycnal diffusivity (K_V) on γ^n = ~28.07 colored on a logarithmic scale. Average diffusivity across the basin K_V = 3.56 * 10^{-5} m^2s^{-1}

Flow across 30°S

Run 0 shows alternating northward, southward and northward flow with depth in the east of the basin above the Vema Channel (Figure 8). The Hunter Gap west of the Rio Grande rise at ~ 32°W shows very weak cyclonic circulation near 3200 dbar. In the interior of the Brazil basin at ~ 30°S,

circulation above ~2000 dbar is northward but circulation from ~2000 dbar to the bottom is dominated by a strong southward current. This southward current weakens towards the MAR.

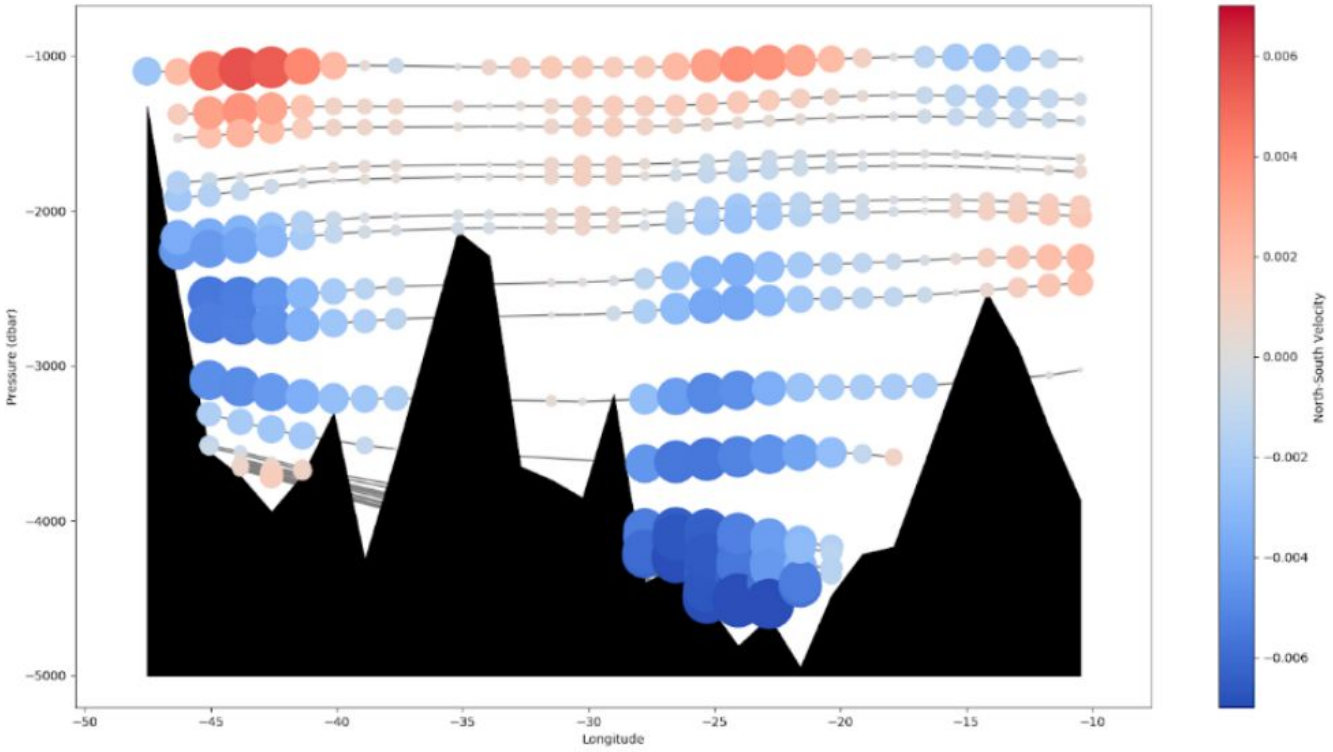

Figure 8. North south velocity across 30°S. The magnitude of each dot is the magnitude of the velocity, the color shows magnitude and direction. Gray lines in background show depth of neutral surfaces.

Net transport across 30°S in Run 0 occurs primarily in AABW is ~10^{10} kg s^{-1} (Figure 9), more than the layers above combined. The transport across 30°S of the top six layers of the model, which includes AAIW and UCDW, shows weak but generally northward transport. In layers six through nine the transport hovers around zero. In the bottommost layers transport is southward throughout the basin (Figure 10). Figure 10 which shows transport instead of accumulated transport like Figure 9 demonstrates the relatively low variability of Run 0 compared to the inverse models of Hernandez-Guerra et al. (2019).

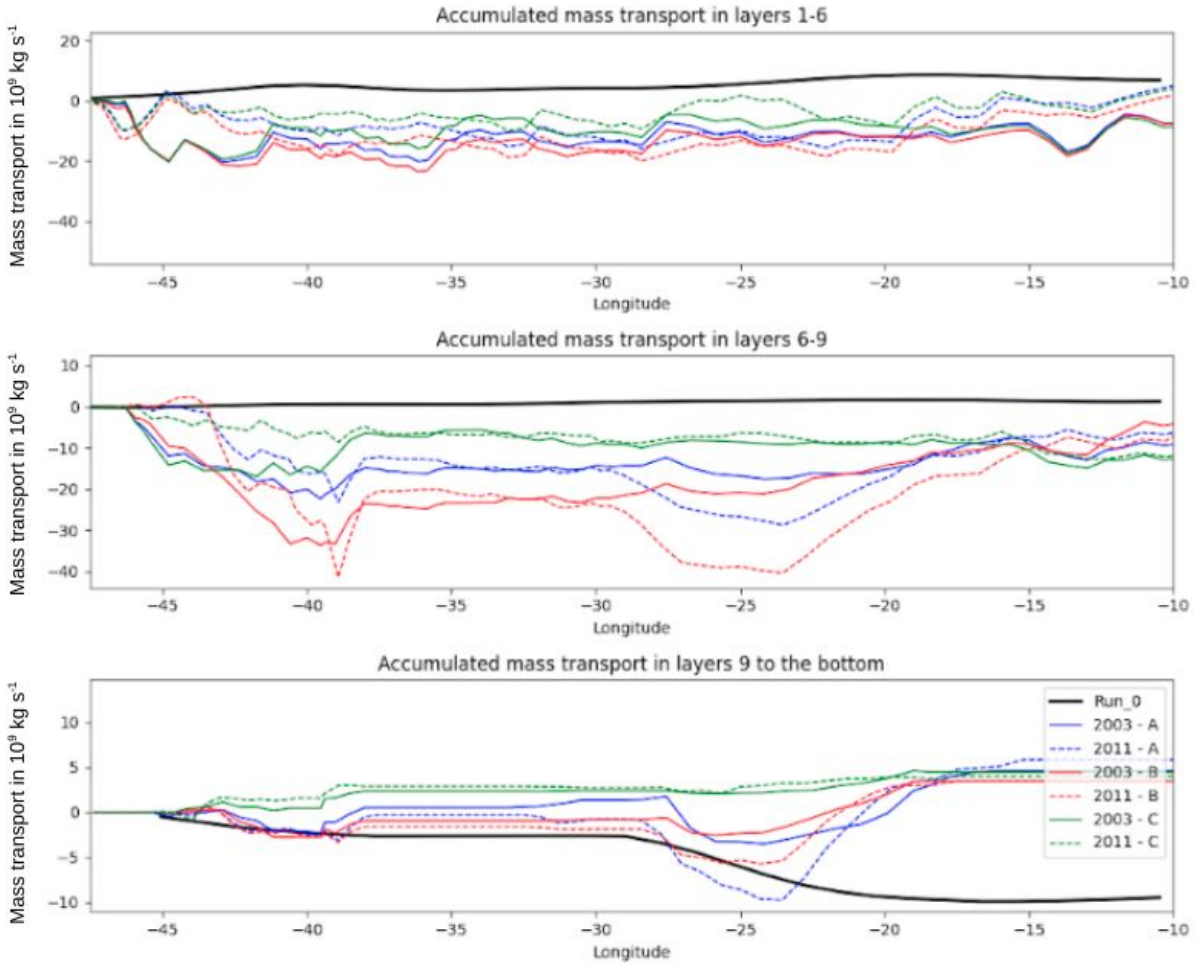

Figure 9. Comparison of accumulated mass transport in Run 0 and the 3 inverse models of Hernández-Guerra across 30°S.

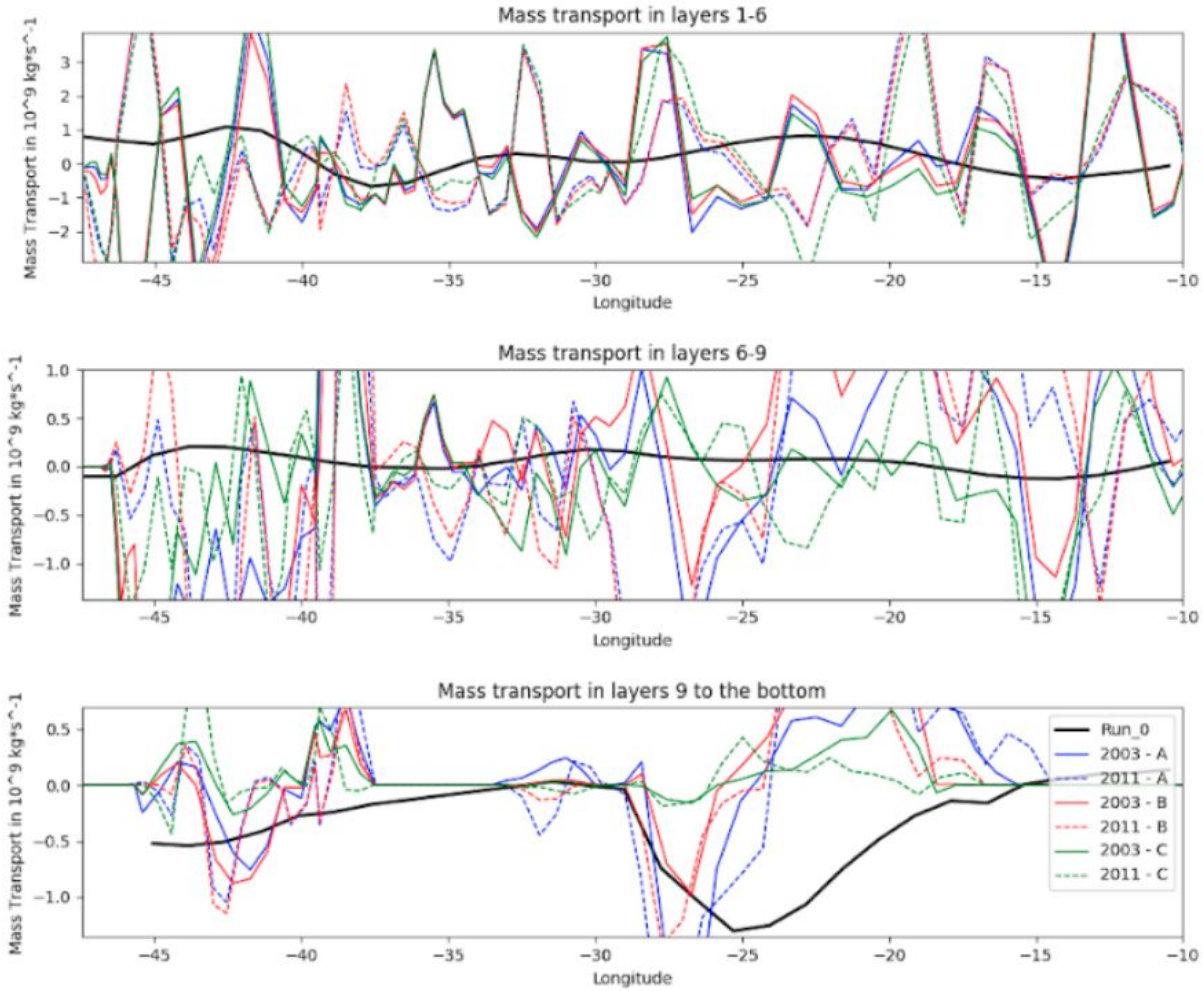

Figure 10. Comparison of mass transport in Run 0 and the 3 inverse models of Hernández-Guerra across 30°S.

Discussion

Lateral circulation

Run 0's solution for absolute geostrophic velocity shows westward flow of AAIW along 26°S until 42°W (Figure 6). This is consistent with the movement of neutrally buoyant floats in the AAIW deployed by Boebel et al. (1997), however, the inverse fails to resolve the boundary currents that drive

floats north and south as they near the edge of the basin .

In AABW the inverse solution shows northward flow through the Vema Channel, which turns east as it exits the channel similar to the schematic circulation of AABW displayed in McDonagh et al. (2002). Unlike the work of McDonagh et al. (2002) which shows an eastward flow south of the Rio Grande rise, a cyclonic circulation around the Rio Grande rise in Run 0 leads to westward flow south of the rise (Figure 6). This is consistent with the westward abyssal circulation south of the Rio Grande rise suggested by water mass properties, including CFC data, and seafloor mud wave features (Coles et al. 2007). Similarly, WOCE section A23 shows that lines of constant neutral density slope downward into the Rio Grande Rise at 30°S implying westward circulation if a medium depth (~2500m) reference level is selected (Koltermann et al. 2011).

Mixing

Run 0's solution for diapycnal diffusivity is consistent with the direct measurements of Polzin et al. (1997) and Kunze (2017) in the interior of the basin, and shows a similar pattern of increasing diffusivity towards the boundaries of the basin (Figure 7). Run 0's calculated diapycnal diffusivity is about an order of magnitude larger than diffusivity values found in the Northeast Pacific basin by Hautala (2018), most likely due to the increased roughness of the Brazil Basin. The lateral diffusivity is similar to that of Hautala (2018). In Run 0 there are a significant amount of negative diffusivity values in the solution caused by a need for potential vorticity to decrease following the flow. For further discussion of negative diffusivity values see Hautala (2018).

Transport Across 30°S

The inverse model in this paper presents a different picture of mass transport across 30°S than the inverse models presented in Hernandez-Guerra et al. (2019). The first large difference is in the

magnitudes of accumulated transport in the upper and middle layers. All three inverse models presented in Hernandez-Guerra et al. (2019) show a strong western boundary current beginning at 45°W which is unresolved in Run 0 (Figure 9). To the east of the boundary current, Run 0 and the inverses presented in Hernandez-Guerra et al. (2019) show no large differences in accumulated mass transport in the upper layers.

Between 20°W and 24°W two out of the three inverse models of Hernandez-Guerra et al. (2019) show a significant northward transport in the bottom layers of their model which does not appear in Run 0. In Hernandez-Guerra et al. (2019) a northward transport of AABW of ~6.9 Sv throughout the entire basin, and ~4 Sv through the Vema channel are constraints on the inverse solution. These values are taken from Hogg et al. (1999), which used a combination of hydrographic stations and direct current measurements to estimate the transport of AABW through the Vema and Hunter channel. It is worth noting that while Hogg et al. (1999) estimated a northward flow of AABW of 4 Sv through the Vema Channel, and 2.9 Sv Hunter channel, Hernandez-Guerra et al. (2019) imposed a constraint of 6.9 Sv of northward transport throughout the entire Brazil Basin from 45°W - 15.3°W. The end result is a southward flow of AABW between 24°W and 28°W in all three inverse models presented in Hernandez-Guerra et al. (2019). Run 0 does show increasingly weak southward velocity towards the MAR, and even a glimmer of northward velocity (Figure 10), but nowhere near the return northward flow seen in Hernandez-Guerra et al. (2019). While Run 0 and the models of Hernandez-Guerra et al. (2019) agree about southward flow between 24°W and 28°W they ultimately paint different pictures of the fate of AABW in the Brazil basin. Hernandez-Guerra et al. (2019) suggests that the AABW that flows south between 24°W and 28°W is recirculated within the basin itself over the western flank of the Mid-Atlantic Ridge, while Run 0 suggests it instead feeds a westward flow along the southern flank of the Rio Grande Rise in the Argentine Basin.

Contrary to both Run 0 and the inverse models of Hernandez-Guerra et al. (2019), Speer and Zenk (1993) computed a northward transport of 6.7 Sv between 40°W and 27°W using a 2°C reference level. This contradicts the broad southern flow of Run 0 at this depth and the strong southward and northward circulation of the inverse models of Hernandez-Guerra et al. (2019). As Speer and Zenk (1993) note, the specific value of northward transport across 30°S has large ramifications on the overall budget of AABW and the implied diapycnal mixing. Broad northward transport throughout the Brazil basin requires a greater magnitude of diapycnal mixing in the interior of the basin than broad southward transport or some kind of recirculation. Direct measurements within the basin are required to better understand the circulation and mixing in the interior of the basin.

The inverse models presented in Hernandez-Guerra et al. (2019) also all show a much more spatially variant picture of transport across 30°S then Run 0 (Figure 10). This is most likely due to the time frame over which each inverse model is run. This paper's inverse model considers a temporal and spatial mean field from multiple decades of observations, while the inverse models of Hernandez-Guerra et al. (2019) each consider a single cruise line. This means that the estimates of transport presented in Hernandez-Guerra et al. (2019) resolve much smaller mesoscale features than our inverse model. A single cruise line also aliases the vertical displacement of isopycnal surfaces caused by internal waves and aliases them into geostrophic flows. This is most apparent when comparing the mass transport of Run 0 and the models of Hernandez-Guerra et al. (2019) (Figure 10).

Conclusion

The majority of transport in the interior of the Brazil Basin across 30°S occurs as southward flow of bottom water. There is northward transport of AABW through the Vema Channel but this is dwarfed by a much larger southward transport to the east of the Rio Grande rise. There is certainly northward circulation of the densest part of the AABW through the Vema and Hunter Channel in boundary currents

that have been observed, but these are unresolved by the inverse model because of their smaller scale dynamics. The dominant feature of circulation in the AABW is a cyclonic circulation around the Rio Grande Rise which transports water south throughout the main basin and recirculates it through the Vema Channel.

The amount of transport of AAIW, UCDW, and NADW is significantly smaller than that found by other models of the region. The magnitude of transport of AABW in Run 0 is similar to that of the inverse models of Hernandez-Guerra et al. (2019). Run 0 and the inverse models of Hernandez-Guerra et al. (2019) also both suggest a strong southern flow along the eastern flank of the Rio Grande Rise, but where Run 0 drives this circulation westward along the southern flank of the Rio Grande Rise, the inverse models of Hernandez-Guerra et al. (2019) recirculate this transport within the Brazil Basin itself through a strong northward return flow along the western flank of the MAR. There is some supporting evidence for westward flow south of the Rio Grande Rise (as required by the inverse model's cyclonic circulation around this feature) in CFC and seafloor mud wave features (Coles et al. 2007). However, analysis of the geostrophic flow relative to a 2°C isotherm 30°S found only northward transport from 40°W - 25°W (Speer and Zenk 1993).

The inverse finds rates of mixing in the basin that are consistent with direct measurements, but high relative to the Northeast Pacific basin where this method was previously applied. This difference in mixing rates between the two basins is consistent with direct measurements done by Kunze (2017). The average diapycnal diffusivity of Run 0 is also consistent with the average diapycnal diffusivity rate measured in the Brazil Basin by Rye et al. (2012) in a tracer release study.

Additional full-depth profiles throughout the Brazil basin would enable a better constrained inverse and help settle the discrepancies between models in the region. The new Deep Argo observing system will greatly increase the spatial and temporal coverage of profiles of temperature, salinity, and

pressure down to 6000 dbar. The utility of the Deep Argo data will be limited by the accuracy of their salinity sensors. However, the inverse technique here is ideally suited to leverage Deep Argo's relatively uniform spatial coverage to produce estimates of interior abyssal circulation, outside the Deep Western Boundary Currents, in basins around the world.

Acknowledgements

The author would like to thank Professor Susan Hautala and Professor Mark Warner both for their help, as well as my classmates in senior thesis for their peer reviews. Data provided by Professors Hernández-Guerra and Talley was instrumental in creating comparisons to their work.

References

Boebel, O., C. Schmid, and W. Zenk. 1997. Flow and recirculation of Antarctic Intermediate Water across the Rio Grande Rise. J. Geophys. Res.: Oceans 102: 20967–20986. doi:10.1029/97JC00977

Coles, V. J., M. S. McCartney, D. B. Olson, and W. M. Smethie. 1996. Changes in Antarctic Bottom Water properties in the western South Atlantic in the late 1980s. J. Geophys. Res. 101: 8957–8970. doi:10.1029/95JC03721

Hautala, S. L. 2018. The abyssal and deep circulation of the Northeast Pacific Basin. Prog. Oceanogr. 160: 68–82. doi:10.1016/j.pocean.2017.11.011

Hernández-Guerra, A., L. Talley, J. L. Pelegrí, P. Vélez-Belchí, M. O. Baringer, A. M. Macdonald, and E. L. McDonagh. 2019. The upper, deep, abyssal and overturning circulation in the Atlantic

Ocean at 30°S in 2003 and 2011. Prog. Oceanogr. 176, 102136. doi:10.1016/J.POCEAN.2019.102136

Hogg, N. G., and W. Brechner Owens. 1999. Direct measurement of the deep circulation within the Brazil Basin. Deep Sea Res., Part II 46: 335–353. doi:10.1016/S0967-0645(98)00097-6

Hogg, N. G., G. Siedler, and W. Zenk. 1999. Circulation and Variability at the Southern Boundary of the Brazil Basin. Journal of Physical Oceanography 29: 145–157. doi:10.1175/1520-0485(1999)029<0145:CAVATS>2.0.CO;2

Jackett, D. R., and T. J. Mcdougall. 1997. A Neutral Density Variable for the World's Oceans. JOURNAL OF PHYSICAL OCEANOGRAPHY 27: 27.

Katsumata, K.H. 2011. G-YoMaHa (Objectively mapped velocity at 1000 dbar derived from trajectories of Argo floats). JAMSTEC. doi:10.17596/0000103

Koltermann, K.P., V.V. Gouretski and K. Jancke. 2011. Hydrographic Atlas of the World Ocean Circulation Experiment (WOCE). Volume 3: Atlantic Ocean (eds. M. Sparrow, P. Chapman and J. Gould). International WOCE Project Office, Southampton, UK, ISBN 090417557X.

Kunze, E. 2017. Internal-Wave-Driven Mixing: Global Geography and Budgets. Journal of Physical Oceanography 47: 1325–1345. doi:10.1175/JPO-D-16-0141.1

Kunze, E., E. Firing, J. M. Hummon, T. K. Chereskin, and A. M. Thurnherr. 2006. Global Abyssal Mixing Inferred from Lowered ADCP Shear and CTD Strain Profiles. J. Phys. Oceanogr. 36: 1553–1576. doi:10.1175/JPO2926.1

Mazloff, M. R., P. Heimbach, and C. Wunsch. 2010. An Eddy-Permitting Southern Ocean State Estimate. J. Phys. Oceanogr. 40: 880–899. doi:10.1175/2009JPO4236.1

McDonagh, E. L., M. Arhan, and K. J. Heywood. 2002. On the circulation of bottom water in the region of the Vema Channel. Deep Sea Res., Part I 49: 1119–1139. doi:10.1016/S0967-0637(02)00016-X

Morris, M. Y., M. M. Hall, L. C. St. Laurent, and N. G. Hogg. 2001. Abyssal Mixing in the Brazil Basin. J. Phys. Oceanogr. 31: 3331–3348. doi:10.1175/1520-0485(2001)031<3331:AMITBB>2.0.CO;2

Müller, T. J., Y. Ikeda, N. Zangenberg, and L. V. Nonato. 1998. Direct measurements of western boundary currents off Brazil between 20°S and 28°S. J. Geophys. Res.: Oceans 103: 5429–5437. doi:10.1029/97jc03529

Reid, J. L. 1989. On the total geostrophic circulation of the South Atlantic Ocean: Flow patterns, tracers, and transports. Prog. Oceanogr. 23: 149–244. doi:10.1016/0079-6611(89)90001-3

Reid, J. L. 1994. On the total geostrophic circulation of the North Atlantic Ocean: Flow patterns, tracers, and transports. Prog. Oceanogr. 33: 1–92. doi:10.1016/0079-6611(94)90014-0

St. Laurent, L. C. S., J. M. Toole, and R. W. Schmitt. 2001. Buoyancy Forcing by Turbulence above Rough Topography in the Abyssal Brazil Basin. JPO 31: 20.

Stommel, H. 1957. The Abyssal Circulation of the Ocean. Nature 180: 733–734. doi:10.1038/180733a0

Talley, L. D. 2008. Freshwater transport estimates and the global overturning circulation: Shallow, deep and throughflow components. Prog. Oceanogr. 78: 257–303. doi:10.1016/j.pocean.2008.05.001

Trossman, D., L. Thompson, and S. Hautala. 2011. Application of Thin-Plate Splines in Two Dimensions to Oceanographic Tracer Data. JTECH 28: 1522–1538. doi:10.1175/JTECH-D-10-05024.1

Peterson, R. G. 1992. The boundary currents in the western Argentine Basin. Deep-Sea Res., Part A 39: 623–644. doi:10.1016/0198-0149(92)90092-8

Polzin, K. L. 1997. Spatial Variability of Turbulent Mixing in the Abyssal Ocean. Science 276: 93–96. doi:10.1126/science.276.5309.93

Rye, C. D., M.-J. Messias, J. R. Ledwell, A. J. Watson, A. Brousseau, and B. A. King. 2012. Diapycnal diffusivities from a tracer release experiment in the deep sea, integrated over 13 years. Geophysical Research Letters 39. doi:https://doi.org/10.1029/2011GL050294

Wunsch, C. 1978. The North Atlantic general circulation west of 50°W determined by inverse methods. Rev. Geophys. 16: 583–620. doi:10.1029/RG016i004p00583